UNIVERSIDAD DE LOS ANDES

THESIS

Two-Photon Imaging Using Tunable Spatial Correlations

Author:
Juan VARGAS

Supervisor:
Dr. Alejandra VALENCIA

A thesis submitted in fulfillment of the requirements for the degree of Physicist

in the

Quantum Optics
Physics Department

May 15, 2018

Declaration of Authorship

I, Juan VARGAS, declare that this thesis titled, "Two-Photon Imaging Using Tunable Spatial Correlations" and the work presented in it are my own. I confirm that:

- This work was done wholly or mainly while in candidature for a research degree at this University.
- Where any part of this thesis has previously been submitted for a degree or any other qualification at this University or any other institution, this has been clearly stated.
- Where I have consulted the published work of others, this is always clearly attributed.
- Where I have quoted from the work of others, the source is always given. With the exception of such quotations, this thesis is entirely my own work.
- I have acknowledged all main sources of help.
- Where the thesis is based on work done by myself jointly with others, I have made clear exactly what was done by others and what I have contributed myself.

Signed:

Date:

"Nonesenses... later due"

N.N

UNIVERSIDAD DE LOS ANDES

Abstract

Science Faculty
Physics Department

Physicist

Two-Photon Imaging Using Tunable Spatial Correlations

by Juan VARGAS

Two-Photon Imaging is a well studied fenomena, where we take advantage of the diferent correlations in wich the light can be related to recontruct the image of certain objects. In this Thesis use diferent spatial correlations of a SPDC light source, where we change this correlations changing the pump waist.

Acknowledgements

The acknowledgments and the people to thank go here, don't forget to include your project advisor. . . s

Contents

List of Figures

For/Dedicated to/To my…

Chapter 1

Introduction

Imaging is a process that we are doing all the time, we have a pair of optical systems (OS) that are mapping constantly, and doing a recreation of the things around us. This pair of OS is what we call eyes, without them we would be able just to *fell* what surround us, it would be impossible to *see*, to do an *image* of our surroundings. The components of the eye are a well stablished optical system, this OS uses the light that is reflected or scattered from the objects and then comes towards the eye. At the back of the eye, we have a photodetector that is called Retina, it converts the photons into electrical signals that travels through our Brain, where the image is then recovered. Figure 1.1 shows a really simplified schematics of the eye seen as an OS.

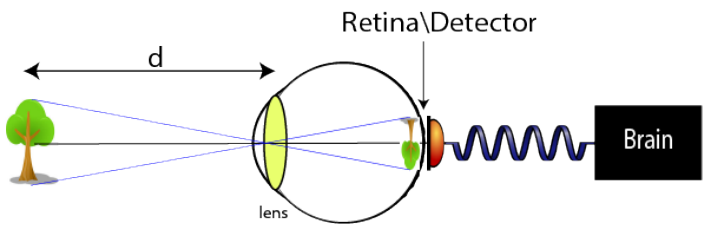

FIGURE 1.1: Eye seen as a Optical System, where d is the distance between object and OS

For taking a photograph of an object, traditionally, we need to face a camera detector for example a CCD to the object, in a way similar to what we do when we point out our eyes to the objects we are seeing, Figure 1.1. Both retina and camera record the spatial shape of the light that comes through. This spatial information is necessary then for the process of reconstructing an image of an object. It is important to point out that when using cameras we usually make images that are 2D representations, of 3D objects. For this reason we talk about an image plane, which is the plane where, depending on the OS, the 2D representation of the object is going to be formed.

What would happen if our retina or camera stopped recording the spatial shape of the light? if our retina now is only able to detect the light that reaches it, but not where it comes from, the imaging process would be impossible, since without spatial information is not posible to create an image. However, Two-photon imaging appears as a techniche that allows to reconstruct images when spatial information of light is absent.

Two-photon imaging started to draw attention after Pittman's first realisation [4]. Figure 1.2 depict a schem of the technique. A light source is divided into two paths. In one path the light is detected by a point like detector D_A that is scanned in the transverse plane. In the other path a lens and an object are followed by a detector D_B that erases the spatial information of the light.The two-photon image is retrieved by correlating the outputs of the detectors D_A and D_B.

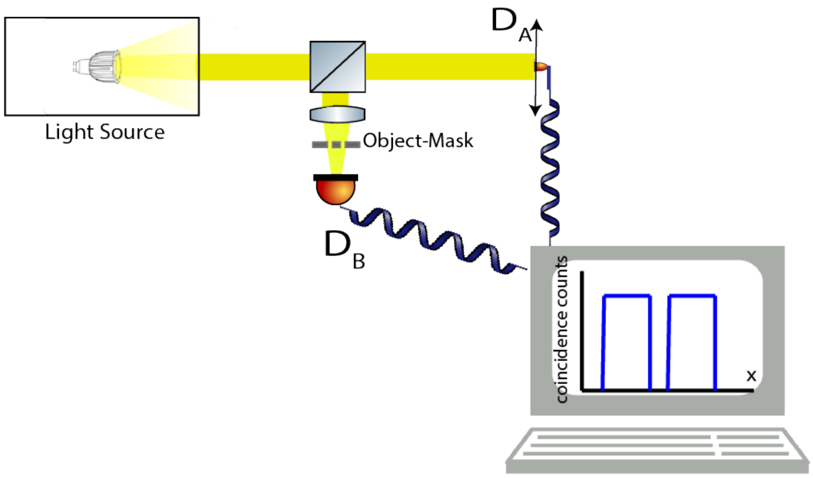

FIGURE 1.2: Two-photon imaging techniche setup

There are different types of Two-photon imaging, and they differ from each other in the nature of the light source used. The first two-photon imaging realisation, done by Pittman in 1995[4], used entangled photon pairs as the light source. The second kind uses chaotic light. This light can be understood as the radiation coming from a blackbody at thermal equilibrium. Valencia *et al.* where the first ones to present an experimental demonstration of two-photon ghost imaging with thermal-like sources[3].

It is possible to reconstruct the image in this two experiments because there is some kind of correlation between the momentum of photons that are generated from the source. For the experiment with the quantum light source, the photons from a pair have negative momentum correlation. In the experiment of the chaotic light, the pair of photons present a positive correlation[5].

Historically to study the effect of Two-photon imaging with different light sources was motivated by the question about the role of entanglement in the generation of the image. However, the role of different types of momentum correlations was not considered at that time. Recently Zhong *et al.* presented a theoretical study of the effect of different types of momentum correlations on Two-photon imaging[6]. In this monograph, we present an experiment in which it is possible to observe the effects of different types of momentum correlations on the generations of Two-photon imaging. We report preliminary results that pave the way for a more complete study that will be *pursue* by the Quantum Optics group.

In our experiment, we have done a Two-photon imaging in what is called a "lens-less two-photon image" configuration[7]. We use a source of entangled photons to which it is possible to tune the transverse momentums correlations. The pair of photons are created by using the nonlinear optical process of spontaneous parametric down conversion (SPDC) in which a laser beam is focused into a nonlinear crystal, and occasionally pairs of photons are produced. Interestingly, the geometry we used for the SPDC configuration allows us to tune the momentum correlations by adjusting the waist of pump beam[8].

This document is organized as follows: Chapter 2 presents a theoretical discussion about the fundamental aspects of the two-photon imaging, and the control of spatial correlations when using a SPDC source. In chapter 3 there is a meticulous explanation of the experimental setup used in this monograph, and its different steps. The experimental results are presented in chapter 4 and finally, conclusions and perspectives are discussed on chapter 5.

Chapter 2

Theory

In Here, we will discus some important facts to get a complete understanding of the physical phenomena of correlations and Two-photon imaging. Specifically, we will develop the notions that are crucial in the understanding of the Two-photon imaging using entangled light. We will star describing the process of SPDC, that provides us with the light source . Then we'll review the phenomena of imaging, looking at the standar version and the Two-photon version.

2.1 Correlations between two photons

The term "correlation" is crucial at this point, and it refers to the relation that two or more situations have. For example we can establish a correlations between the US dolar currency exchange rate and the prices of technology in one country. These two things have direct relation, if one blows up, the other one will too. These two situations, or variables, can have a strong correlations or a weak one.

Indeed in quantum physics we can have a pair of photons that are so strongly and specially correlated, in their possible degrees of freedom (spatial, temporal and polarization), that we say they are entangled. This statment can leads us to a dense discussion about the nature of this entanglement, a discussion that were started between Einstein and Bohr in the first years of quantum physics [9].

For the topic of this monograh it is relevant to have a pair of spatially correlated photons. This can be conveniently produced by the process of SPDC. This produces photons that are indeed entangled. However, we are not interested in this feature, Since in order to observe two photon imaging only the spatial correlations are needed.

2.1.1 Spontaneous Parametric Down Conversion

As the title of this work implies, we need a light source that produces pair of photons, and we would like to exploit the advantages of strong correlations between them. The photons generated via spontaneous parametric down conversion (SPDC) are widely used in quantum optics experiments. The popularity of this source of paired photons is strongly related to the relative simplicity of its experimental realisation, and to the variety of quantum features that down converted photons can exhibit. The generated photons via SPDC can be correlated in different degrees of freedom, for example in polarisation, in frequency, in orbital angular momentum and in transverse momentum [10].

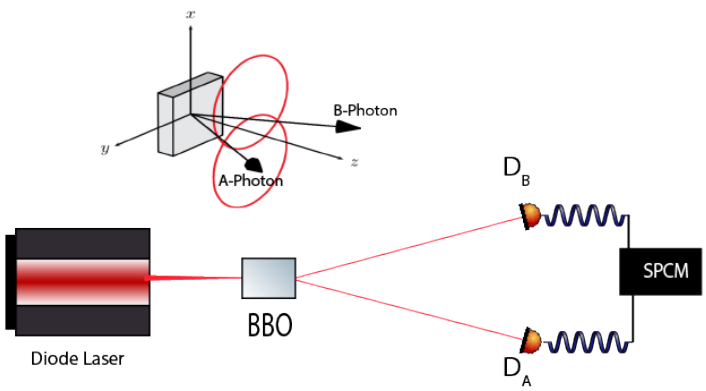

FIGURE 2.1: Simple Experimental setup for the type-II non-collinear SPDC process

SPDC is an optical process in which a pump beam propagating in the z-direction is focused into a nonlinear crystal of length L. Depending on the polarisation direction of the produced photons, the nonlinear crystals can be classified in types. The type-0 crystal will produce pairs that are polarised in the source light direction. The type-I will produce pairs that are polarised in the perpendicular direction of the pump. The last type, type-II crystals will produce a pair of photons, one with the polarisation in the same direction as the pump, and the other one in the perpendicular direction. This procces can also be clasified according to the geometry, the relative direction from the crystal, in which the pair of down converted photons are going to be generated. The generated pair can emerge from the crystal in a collinear or non-collinear configuration. In Figure **??** the non-collinear configuration is shown, where light is generated in two separated cones, for each polarisation, these light cones intercepts in two places, from where we will use pair the pair A-photon and B-photon.

For the rest of this monography we will be focused in the type-II and non-collinear configuration. Using first order perturbation theory and the paraxial approximation, the two-photon state coming out from the crystal, $|\Psi\rangle$, is given by [8] type-II:

$$|\Psi\rangle = \int d\vec{q}_B d\vec{q}_A d\Omega_B d\Omega_A \times [\Phi(\vec{q}_B, \Omega_B; \vec{q}_A, \Omega_A)\hat{a}^\dagger(\Omega_B, \vec{q}_B)\hat{a}^\dagger(\Omega_A, \vec{q}_A) \\ + \Phi(\vec{q}_A, \Omega_A; \vec{q}_B, \Omega_B)\hat{a}^\dagger(\Omega_B, \vec{q}_B)\hat{a}^\dagger(\Omega_A, \vec{q}_A)] \, |0\rangle \, . \tag{2.1}$$

Where this state function depends on the transverse wave vectors $\vec{q}_n = (q_n^x, q_n^y)$ and frequency detuning, $\Omega_n = \omega_n - \omega_0^n$, around the central frequencies, ω_0^n, for the photon at the path A or B ($n = A, B$). The $\Phi(\vec{q}_B, \Omega_B; \vec{q}_A, \Omega_A)$ and $\Phi(\vec{q}_A, \Omega_A; \vec{q}_B, \Omega_B)$ are the mode functions or biphotons that contains all the information about the correlations between the pair of down-converted photons. The operator $\hat{a}^\dagger$ indicates the creations of an n-polarized photon with transverse momentum $\vec{q}_n$, and frequency detuning Ω_n.

For the light source that we will usea in this monograph it is enough just one of the biphotons of the Eq. 2.1. As it will shown later this later this corresponds to put a pair of polarisers before the detection of the light. The Two-photon state reduces to:

$$|\Psi\rangle = \int d\vec{q}_B d\vec{q}_A d\Omega_B d\Omega_A \times [\Phi(\vec{q}_B, \Omega_B; \vec{q}_A, \Omega_A)\hat{a}^\dagger(\Omega_B, \vec{q}_B)\hat{a}^\dagger(\Omega_A, \vec{q}_A)] \, |0\rangle \, . \tag{2.2}$$

The mode function $\Phi(\vec{q}_B, \Omega_B; \vec{q}_A, \Omega_A)$ is related with the joint probability of detecting both an B-polarized photon, with tranverse momentum $\vec{q}_B$ and frequency detuning Ω_B, at the detector B and an A-polarized photon, with tranverse momentum $\vec{q}_A$ and frequency detuning Ω_A, at the detector A.

2.1.1.1 Phase matching conditions

In particular, $\Phi(\vec{q}_B, \Omega_B; \vec{q}_A, \Omega_A)$ reads [8]:

$$\Phi(\vec{q}_B, \Omega_B; \vec{q}_A, \Omega_A) = \mathcal{N}\alpha(\Delta_0, \Delta_1)\beta(\Omega_B, \Omega_A) \times sinc\left(\frac{\Delta_k L}{2}\right) e^{i\frac{\Delta_k L}{2}} . \tag{2.3}$$

Where $\mathcal{N}$ is a normalisation constant, $\alpha(\Delta_0, \Delta_1)$ and $\beta(\Omega_B, \Omega_A)$yields the informations of the pump's transverse and spectral distribution, respectively, L is the length of the nonlinear crystal. For the process that is happening inside the crystal, there are some conditions that have to be fulfilled. These conditions are related with the energy and momentum conservations inside the parametric down conversion process. The terms Δ_0, Δ_1 and Δ_k are functions that result from the phase matching conditions and read:

$$\Delta_0 = q_B^x + q_A^x. \tag{2.4}$$

$$\Delta_1 = q_A^y cos\phi_A + q_B^y cos\phi_B - N_B\Omega_B sin\phi_B + N_A\Omega_A sin\phi_A - \rho_B q_B^x sin\phi_B. \tag{2.5}$$

$$\begin{aligned} \Delta_k = N_p(\Omega_B + \Omega_A) - N_B\Omega_B cos\phi_B - N_A\Omega_A cos\phi_A \\ -q_B^y sin\Omega_B + q_A^y sin\Omega_A + \rho_p\Delta_0 - \rho_B q_B^x cos\phi_B. \end{aligned} \tag{2.6}$$

The angles ϕ_B and ϕ_A are the creation angles of the down- converted photons with respect to the pump's propagation direction, whereas ρ_p and ρ_B are angles, they account for the walk-off of the pump p and the B down- converted photon, respectively. $N_n = \frac{\delta k}{\delta\omega}$ denotes the inverse of the group velocity for each photon.

2.1.2 Spatial Correlations

In order to observe the correlations presented in 2.3 we have to take into account some considerations about the descrption of the things we have in optical table. First of all we have a pump beam with a Gaussian profile with waist w_p in such way that $\alpha(\Delta_0, \Delta_1) \propto \exp[-w_p^2(\Delta_0^2 + \Delta_1^2)/4]$, a CW pump laser, mathematically represented by $\beta(\Omega_B, \Omega_A) \propto \delta(\Omega_B + \Omega_A)$. Making the aproximations for the sinc function by a Gaussian fuctions with the same width at $1/e^2$ of its maximum, i.e., $sinc(x) \approx \exp(-\gamma x^2)$ with γ equal 0.193. The mode function reduces to:

$$\begin{aligned} \Phi(\vec{q}_B, \Omega_B; \vec{q}_A, \Omega_A) = \mathcal{N}\beta(\Omega_B, \Omega_A)\times \\ exp\left[-\frac{w_p^2(\Delta_0^2 + \Delta_1^2)}{4} - \gamma\left(\frac{\Delta_k L}{2}\right)^2 + i\frac{\Delta_k L}{2}\right]. \end{aligned} \tag{2.7}$$

As said before, we are interested in the spatial correlation that the photons exhibit. For these reason the frequency information has to be traced out. This is achieved by placing some interferometer filters before detection. This spectral filters are modeled as $f_n(\Omega_n) = \exp[-\Omega_n^2/(4\sigma_n^2)]$, with bandwidth

σ_n chosen to achive a regimen where the spatial-spectral correlations are completely broken [11]. To achieve this mathematically we have to integrate 2.7 around the spatial variables:

$$\tilde{\Phi}(\vec{q}_B, \vec{q}_A) = \int d\Omega_B d\Omega_A f_B(\Omega_B) f_A(\Omega_A) \Phi(\vec{q}_B, \Omega_B; \vec{q}_A, \Omega_A). \tag{2.8}$$

The Biphoton then takes a quadratic form[8]:

$$\tilde{\Phi}(\vec{q}_B, \vec{q}_A) = Nexp\left[-\frac{1}{2}x^T A x + i b^T x\right]. \tag{2.9}$$

where N is a normalization constant, that satisfies $\int\int |\tilde{\Phi}(\vec{q}_B, \vec{q}_A)|^2 d^2\vec{q}_B d^2\vec{q}_A = 1$. x is a 4-dimensional vector defined as $x = (q_B^x, q_B^y, q_A^x, q_A^y)$, A is a 4 x 4 real-valued, symmetric, positive definite matrix and b is a 4-dimensional vector. A and b are defined from the phase-matching conditions of the SPDC process. x^T and b^T denote the transpose of x and b. A and b are functions that depend of all the relevant parameters in the experiment such as the length of the crystal L, pump waist w_p, creation angles inside the crystal φ_n and the width of the spectral filter σ_n.

is pearson coeficient realted to correlations parameter ???

Figures/theoricalxx.png

Figures/theoricalyy.png

FIGURE 2.2: Experimental Spatial correlations between a pair of down-converted photons. Right image shows the correlation in the x variable. Left shows the correlation in the y variable, Beam propagating in the z direction

Figure 2.2 show a couple of examples, of how these correlations we are talking about look like. These correlations have elliptical shape, and show how strong is the posibility of detecting a photon at a given momentum, looking at XX Correlation, there is a great chance of detecting simultaneously a photon at $q_B = 0$ and at $q_A = 0$. Now if we look at the left graph, it is showing the correlation of the pair of photons in the y direction, there is a significant probability of measuring simultaneously a photon at $y_B = 0.4$ and at $y_A = -0.4$. It is interesting how in this case there is a "negative" correlation, the expected position at which we will find the other photon, is at the same, but negative position. Another interesting fact we have to point out, is that this correlations algo can be sharper, the x correlation have a more circular shape, making wider the posible values for a given x_B. In contrast the y correlation is more eliptic, meaning it restring the posible values por a given y_B. It is easy to think how a strong correlation should look like, a strong correlations in spatial variables would mean that if we have the position of one photon at the position $\vec{q}_B$ we immediately would know which $\vec{q}_A$ have the other photon, this king of ideal spatial correlation would look like a straigth line really thin, Figure 2.3, and it would be like having a relation of like $\delta(\vec{q}_b - \vec{q}_a)$.

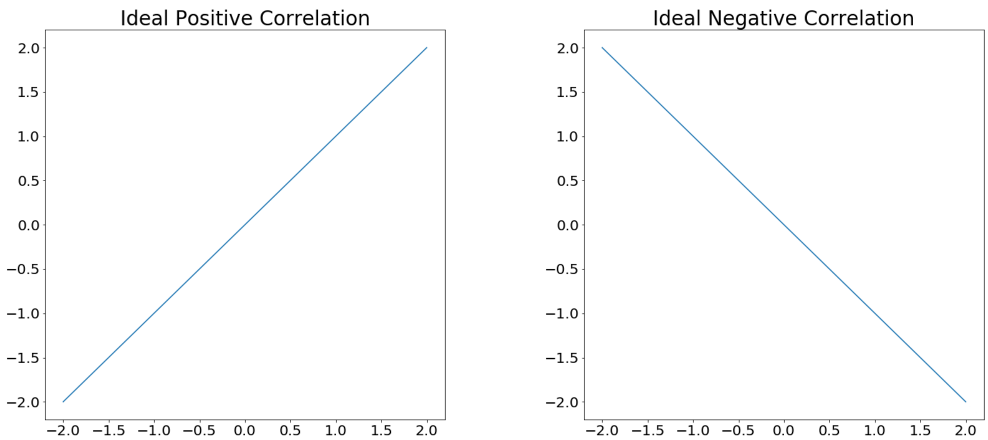

FIGURE 2.3: Positive and Negative ideal spatial correlations

2.1.3 Tunable Spatial Correlation SPDC source light

It is clear that both 2.7 and 2.8 depend on w_p, the pump waist. If we change this parameter and keep the rest of the parameters constant, the term in the exponential function $[-w_p^2(\Delta_0^2 + \Delta_1^2)/4]$ will variate, making changes in the shape of the original mode function. As it was mentioned here before and in [8], the mode function contains all the informations about the correlations of the generated down converted photons. Hence changing the pump waist w_p will change the correlations of the generated pair of photons.

Figures/correlationsWaist.png

Figures/correlationsWaist2.png

FIGURE 2.4: simulated correlations

2.2 Imaging

As said in the Introduction, imaging is a process in which we make a reconstruction of an object using the spatial information of the light that where reflected, or scattered from that object. This representation of the object can not be an exact copy, all kind of blurry things we can see when forgetting our glases. The diference between having or not our glasses is that they will bost up our spatial resolution of the object.

2.2.1 Standar Imaging

The concept of optical imaging was well developed in classical optics and the Figure 2.5 schematically illustrates a standar imaging setup. In this setup an object is illuminated, an imaging lens is used to focus the scattered and reflected light from the object onto an image plane which is defined by the "Gaussian thin lens equation"[12]:

$$\frac{1}{S_o} + \frac{1}{S_i} = \frac{1}{f}, \tag{2.10}$$

where S_o is the distance between the object and the imaging lens, S_i the distance between the imaging lens and the image plane, and f the focal lenght

of the imaging lens. This equation defines a point-to-point relationship between the object plane and the image plane: any radiation starting from a point on the object will colapse at a certain point at the image plane.
This one-to-one correspondence in the image-forming relationship between

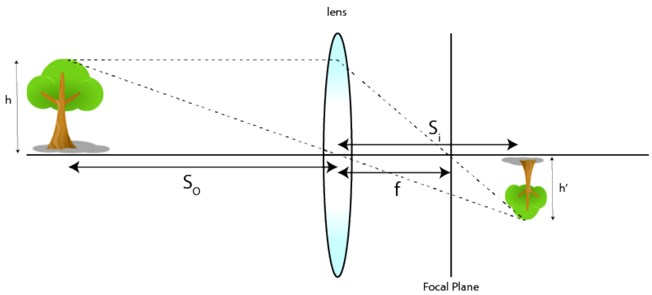

FIGURE 2.5: Optical imaging: a lens produces an image on an object at S_i. This distance is defined by the Gaussian thin-lens equation

the object and the image planes produces a perfect image. The observed image can be magnified or demagnified, for example, in the Figure 2.5 the original object is a tree, and it is demagnified at the image plane. This depends on which optical system are we using, what kind on lenses are involved and the distance between object and them.

The observed image is a reproduction of the illuminated object, mathematically corresponding to a convolution between the object distribution fuction $|T(\vec{r_o})|^2$ (aperture function) and a δ-function, which is present for the perfect point-to-point correspondence [13]:

$$\langle I(\vec{r_i})\rangle = \int_{obj} d\vec{r_o}|T(\vec{r_o})|^2\delta(\vec{r_o} + \frac{\vec{r_i}}{m}), \tag{2.11}$$

where $\langle I(\vec{r_i})\rangle$ is the mean intensity at the image plane, $\vec{r_o}$ and $\vec{r_i}$ are 2-D vectors of the transverse coordinates, $\vec{r_n} = (x_n, y_n)$, in the object and image planes, respectively, and $m = s_i/s_o$ is the image magnification factor.

In reality, we are limited by the finite size of the optical system, we may never obtain a perfect image. The incomplete constructive-destructive interference turns the point-to-point correspondence into a point-to-"spot" relationship. The δ-function in the convolution of equation 2.11 will be replaced by a point-to-"spot" image-forming function, or a point-spread function,

$$\langle I(\vec{r_i})\rangle = \int_{obj} d\vec{r_o}|T(\vec{r_o})|^2\text{somb}^2[\frac{\pi D}{\lambda S_o}|\vec{r_o} + \frac{\vec{r_i}}{m}|], \tag{2.12}$$

where the sombrero-like point-spread function is defined as $\text{somb}(x) \equiv 2J_1(x)/x$, with $J_1(x)$ the first-order Bessel function, D the diameter of the imaging lens and λ the wavelength of the light used. the finite size of the spot is defined by $J_1(x)$ and determined by the ratio $D/\lambda S_o$.

This finite size of the spot in the point-to-"spot" relationship we described before, is what is called spatial resolution. A higher spatial resolution of the image is achieved by the conditions described before.

Another daily situation in which we are forming images, is when we take a picture. Cameras manufacteres play with this functions to achieve a high spatial resolution, a spot-to-pixel correspondence. For further informations about this "real life" situation check[13] chapter 4 for further development.

2.2.2 Two-photon Imaging

Two-photon imaging consist in reconstructing an image of an object. But in this case we use two dectector located in the two differents paths of the light. By looking at the individual signal from each detector we get a constant signal, with no information about the object, Figure 2.6. But if instead we look at the intensities correlations of both detectors we retrive the image of the object.

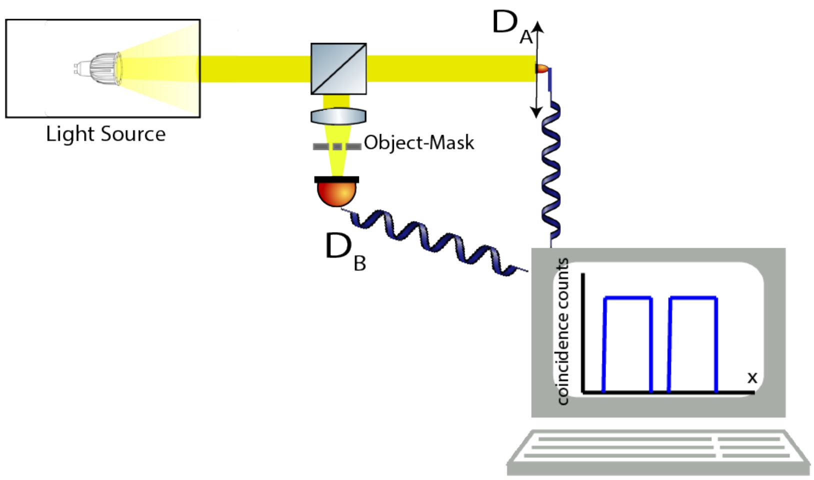

FIGURE 2.6: Simple schematic for the Two-photon Imaging, two slite used OIHASUOIASUD COMPLETE

In order to reconstruct the image of the object, we have to introduce some kind of spatial dependence, the object, is distributed along a transverse direction of the light propagation. But what we have learnt is that scanning along the x-direction (asuming that light propagates along the z-direction), in the path that have no interaction with the object D_A, and colecting all the light that interacts with the object D_B, gathering no spatial information. We reconstruct the double slit in the coincidences counts, every time we have a photon detected going througt the double slit, and a photon at a certaint position x_i, we graph coincidences vs x_i and we get the image of the double slit, Figure 2.6. REWRITE !!!!!!!!

The standar imaging used the photons at the image plane, to form the image. In other words it measures one photon per spot at the image plane. For the two-photon imaging, in certain aspects the behaviour is similar as that of the classical. They both exhibit a similar point-to-point imaging-forming function, except the two-photon image is only reproducible in the joint-detection between two independent photodetectors, and the point-to-point imaging-forming function is in the form of second-order correlation,

$$R_{BA}(\vec{r_A}) = \int_{obj} d\vec{r_B} |T(\vec{r_B})|^2 G^{(2)}(\vec{r_B}, \vec{r_A}), \tag{2.13}$$

where $R_{BA}(\vec{r_B})$ is the joint-detection counting rate between photodetectors D_B and D_A. $G^{(2)}(\vec{r_B}, \vec{r_A})$ is a second-order correlation function, corresponding to the probability of observing a joint photo-detection event at the coordinates $\vec{r_B}$ and $\vec{r_A}$. The physics behing $G^{(2)}(\vec{r_B}, \vec{r_A})$ is what changes between depending of the light source used.

This second-order correlation functions is defined as[13]:

$$G^{(2)}(\vec{r_B}, \vec{r_A}) = \frac{\langle E^*(\vec{r_B}) E^*(\vec{r_A}) E^(\vec{r_B}) E^(\vec{r_A}) \rangle}{\langle |E^(\vec{r_B})|^2 \rangle \langle |E^(\vec{r_A})|^2 \rangle}. \tag{2.14}$$

where E is bla bla PUT SOBRERO

2.2.2.1 LenslessTwo-photon Imaging using entangled photon

In the previous section we introduced the notion of two-photon imaging , but we didn't care much about the nature of the source light. For this monograh we will use entangled photon as the source light. For now on we will focus on decribing the experimental setuo in fig ,, lensless, objectfourier plane, lensless

The main point of the section is to calculate Eq 2.13 for this situation, we need to know the state of the biphoton at the output of the crystal reference the equation:

$$\tilde{\Phi}_c(\vec{q}_c, \vec{q}_c) = N e^{\left[-\frac{1}{2} x^T A x + i b^T x\right]}. \tag{2.15}$$

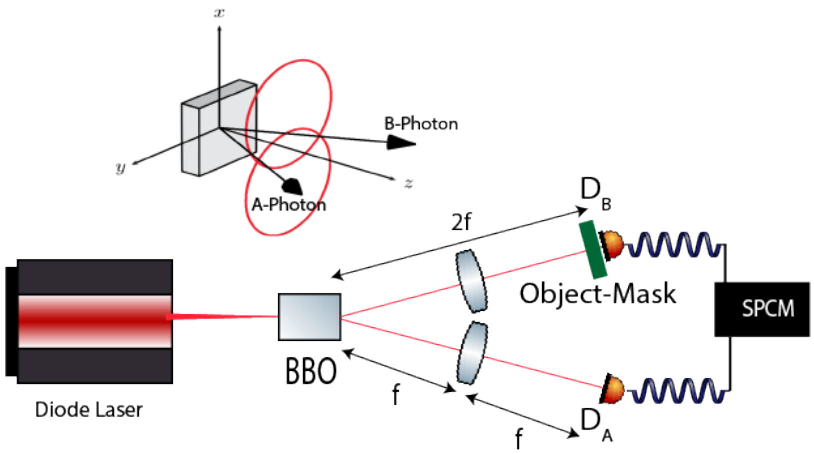

FIGURE 2.7: Simple schematic for a Two-photon Imaging using entangled photons and a 2-f system

Then from this result we can use the fresnel propagation theory to analytically model the biphoton propagation in any arbitrary Two-photon Imaging/Lensless Two-photon Imaging setup.This propagation is done by determining the Green function of the optical path by which the beams will travel[].

Since both path A and B have an identical 2-f system, we are at the called Fourier plane. It is well know that when the light goes through this system suffers a Fourier transform[13]. It means that if , there is a relation beetwen the initial q_c initial transverse momentum at the crystal, and the r_f final position of the photons. This relation is:

$$\vec{q}_{initial} = \frac{2\pi}{\lambda f}\vec{r}_{final}, \tag{2.16}$$

where $\vec{q}_{initial}$ is the transverse momentum of the light before the 2-f system, $\vec{r}_{final}$ is the position of photon after going through the lens and traveling a 2-f distance. f stands for the focal length of the lenses used and λ wavelength.

The Green function that propagates light with transverse momentum $\vec{q}$ from the source, to the Fourier plane located at a position $\vec{r}_f$ is[14]:

$$G(\vec{q}, \vec{r}_f) = \int d^2\vec{r}_l \int d^2\vec{r}_c h(\vec{r}_f - \vec{r}_l, f) L_f(\vec{r}_l) h(\vec{r}_l - \vec{r}_c, f) e^{iq\cdot\vec{r}_c}. \tag{2.17}$$

With $\vec{r}_c$ and $\vec{r}_l$ denoting the transverse position vectors in the plane of the crystal and the lens respectively. $h(\vec{r}_f - \vec{r}_l, f)$ and $h(\vec{r}_l - \vec{r}_c, f)$ are the Fresnel propagators[1] that propagates light from $\vec{r}_l$ to $\vec{r}_f$ and $L_f(\vec{r}) = \Psi(\vec{r}, -f)$ is the

[1]Fresnel Propagator: $h(\vec{r}, z) = (-\frac{i}{\lambda z})e^{(i\frac{2\pi z}{\lambda})}\Psi(\vec{r}, z)$ with $\Psi(\vec{r}, z) = e^{(i\frac{\pi}{\lambda z})\vec{r}^2}$.

thin-lens transfer function associated to a lens[14].
Taking advantage of the 2-f system as a Fourier transform to reduce the amount of calculations , using the relation 2.16, and after solving the integrals over r_l and r_c, equation 2.17 can be written as:

$$G(\vec{q},\vec{r}_f) = Ce^{\frac{i\pi}{\lambda f}\vec{r}_f^2} e^{\frac{i\lambda f}{4\pi}\vec{q}^2} \delta(\vec{q} - \frac{2\pi}{\lambda f}\vec{r}_f), \tag{2.18}$$

where C is a complex constant. Then we can finally propagate the biphoton function in terms of transverse momenta. Where $\Phi_1(\vec{q}_B,\vec{q}_A)$ is the biphoton after traveling through two arbitrary optical paths, it can be expressed in terms of the corresponding Green functions and the initial biphoton function, equation 2.15, $\tilde{\Phi}_c(\vec{q}_c,\vec{q}_c)$ as:

$$\Phi_1(\vec{q}_B,\vec{q}_A) = G_B(\vec{q}_B,\vec{r}_B)G_A(\vec{q}_A,\vec{r}_A)\tilde{\Phi}_c(\vec{q}_c,\vec{q}_c), \tag{2.19}$$

where $\vec{r}_B$ and $\vec{r}_A$ denotes the photon position in the transverse plane at a 2-f distance from the crystal, the subscrip stand for the different path followed by light, Figure 2.7. The $G_B(\vec{q}_B,\vec{r}_B)$ and $G_A(\vec{q}_A,\vec{r}_A)$ are the green functions for each path, defined as in equation 2.18, they are:

$$G_B(\vec{q}_B,\vec{r}_B) = G(\vec{q}_B,\vec{r}_B) \times T(\vec{r}_B). \tag{2.20}$$

$$G_A(\vec{q}_A,\vec{r}_A) = G(\vec{q}_A,\vec{r}_A). \tag{2.21}$$

Where $T(\vec{r}_B)$ is the transfer function of the object, which is only present at the B path, Figure 2.7. Gathering all the previous results we can obtain $\Phi_1(\vec{r}_B,\vec{r}_A)$. This is done by replacing Eq. 2.20 and 2.21 into Eq. 2.19, then evaluating the integrals over the transverse momentums, we obtain:

$$\Phi_1(\vec{r}_B,\vec{r}_A) = C^2 T(\vec{r}_B)\Phi(\frac{2\pi}{\lambda f}\vec{r}_B, \frac{2\pi}{\lambda f}\vec{r}_A). \tag{2.22}$$

This function describes the biphoton at the planes of the object and the scanning detector. It shows that the biphoton at the 2F plane as a function of $\vec{r}_B$ and $\vec{r}_A$. If we take a closer look, this result enable us to compute the biphoton at the 2-f plane by using Eq 2.9 without the need to actually calculate its propagation, just by evaluating it with the Fourier relationship, 2.16. This is specially usefull when we try to simulate this on a computer, the amount of calculations is significantly reduced by this fact.

As described at the beginning of this Section 2.2.2, we lose all the spatial information about the photon that interacts with the Object, and this is done by placing a bucket detector that gathers all light and send it to a multimode optic fiber, without saving any information about the position of the photons in this path B. From the mathematical point of view, the bucket detector is modeled as: $\Phi_1(\vec{r}_A) = C^2 \int d^2\vec{r}_B T(\vec{r}_B)\Phi(\frac{2\pi}{\lambda f}\vec{r}_B, \frac{2\pi}{\lambda f}\vec{r}_A)$. Using the fact that the coincidence counts that will be measured by the Detectors will be proportional to the magnitude square of the resulting biphoton function $\Phi_1(\vec{r}_A)$[13].

$$R(\vec{r}_A) \propto |\int d^2\vec{r}_B T(\vec{r}_B)\Phi(\frac{2\pi}{\lambda f}\vec{r}_B, \frac{2\pi}{\lambda f}\vec{r}_A)|^2 \tag{2.23}$$

Where $R(\vec{r}_A)$ is the function that describes de coincidences counts between de detectors D_B and D_A in Figure 2.7. $R(\vec{r}_A)$ is a function of the spatial positions, (x_A, y_A) of the detection plane at D_A. This function $R(\vec{r}_A)$ have the expected behaviour described by $R_{BA}(\vec{r_A})$ in Eq. 2.13, where the second-order correlation function in this case is $\Phi(\frac{2\pi}{\lambda f}\vec{r}_B, \frac{2\pi}{\lambda f}\vec{r}_A)$, as we said, the function containing all the informations about the correlations between the pair of down-converted photons. Moreover, Equation **??** indicates that the form of $\Phi(\vec{q}_B, \vec{q}_A)$ determines if $T(\vec{r}_B)$ can be recovered in the coincidence count. Additionally, the type of spatial correlation in $\Phi(\vec{q}_B, \vec{q}_A)$ defines the orientation of the image obtained.

2.2.2.2 Effect of the different spatial correlations

Chapter 3

Experimental Setup

In the following chapter we will look in detail the components of the experimental setup and its stages. This experimental setup located on the optical table of the Quantum Optics Laboratory

3.1 SPDC Setup

Following the treatment made in the previous chapter. The first ingredient is the SPDC light, to obtain pair of photons the experimental setup shown in Figure 3.1. From here we will star describing each of the components presented.

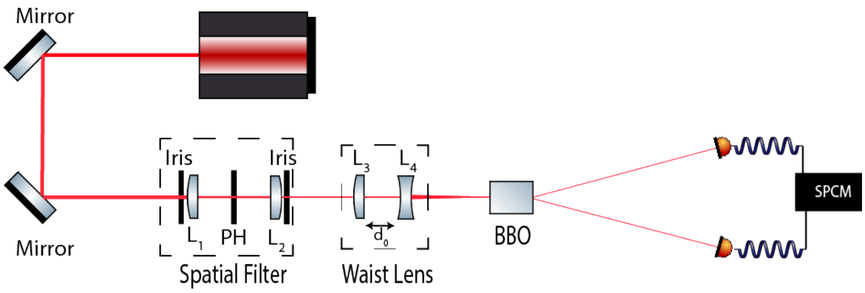

FIGURE 3.1: Experimental Setup for the SPDC light Source

3.1.1 Diode Laser

Before having pair of correlated photons, we start by having a coherent light source, for this experiment we use a Diode Laser that delivers a continuous wave(CW) at $\lambda = 406, 101nm$ and $\Delta\lambda = 4nm$. The laser model No. DL 405-200 delivers light at 200 mW with a beam diameter of 1.5 mm and a beam Divergence[1] 1.2 mrad.

[1]The beam divergence is an angular measure of the increase in beam diameter with distance from the original optical aperture

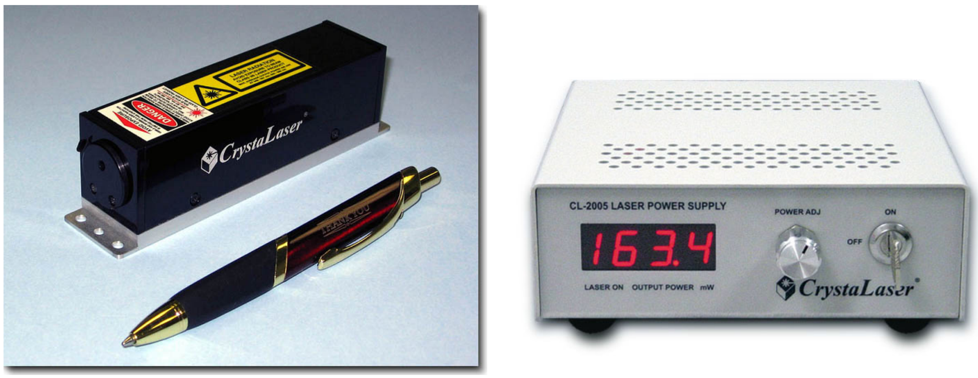

FIGURE 3.2: Image of the Diode Laser and it's control module, Taken from [1]

3.1.2 Mirror

As seen in Figure 3.1 we redirect the laser beam two times, for doing so we use a pair of mirrors. For this kind of experiments, when the efficiency of the optical elements is really important, it is important to use the correct type of mirror, we want a mirror that reflects most of the light. For this reason, depending on the wavelength it is posible to find mirrors and lenses with different types of coating. Mirror and Lenses have a thin layer that is more efective for a range of wave lengths.

In Figure 3.3 we can see a Mirror and the base used to place it, it is posible to manipulate the direction in which the mirror will reflect the light, we can do this by manipulating the screws, each one moves the reflected laser in one direction. In the experimental setup we use two mirror to change the direction two times, this is because using just one could be more complicated when aligning the rest of optical elements. When two mirror are used, we have more possibilities, 4 in total. The advantage of having more possibilities is that the manipulation can be more precise.

3.1.3 Spatial Filter

A laser beam can be characterized by measuring its spatial intensity profile at points perpendicular to its direction of propagation. The spatial intensity profile is the variation of intensity as a function of distance from the center of the beam, in a plane perpendicular to its direction of propagation. In Figure 3.4 we se see the input gaussian beam and how its intensity fluctuates around the x axis. The output desired beam after going through the spatial filter is then shown. The simplest arrangement to achieve this output spatial intensity profile is show in the Figure 3.5, where at the end we have a beam

FIGURE 3.3: Mirror and the cavity mount

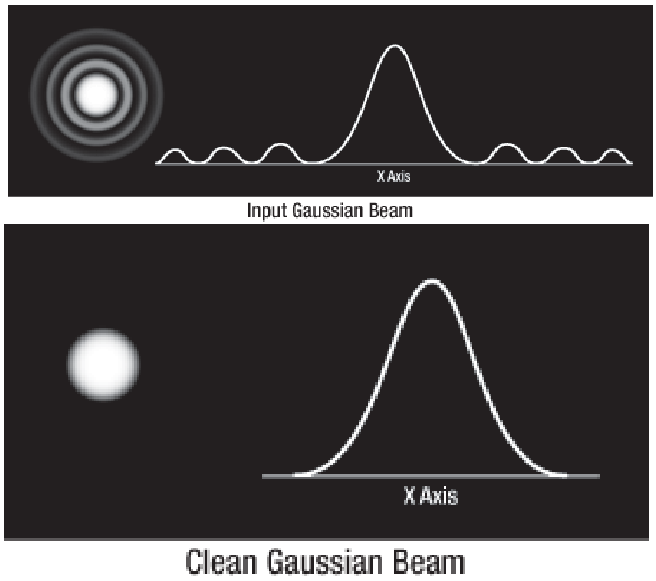

FIGURE 3.4: The spatial intensity profile before and after the spatial filtering process , Taken from [2]

which intensity strength falls off transversely following a bell shaped curve that's symmetrical around the central axis. Taking a closer look at the input

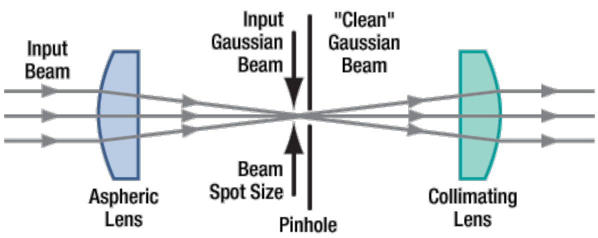

FIGURE 3.5: Basic elements of a Spatial Filter. In our experiment we use a Aspheric Lens of $f = 30mm$(LA1805-A), a pinhole of $50\mu m$ and a collimating lens of $f = 60mm$(LA1134-A). Taken from [2]

Gaussian beam in Figure 3.4 we may recognise a diffraction pattern, the well known Airy disks. However, when we measure this spatial profile directly from the diode laser, we find out that it doesn't follow that behaviour, on the contrary it follows a more random spatial profile. This ramdom spatial profile is a result of the randomnes in the quantum emissions and absorptions that are happening at the exited atoms at the diode laser[12].

In order to have this spatial intensity profile at the input of the lens arrangement, Figure 3.5, we put a circular aperture with the help of a iris, Figure 3.6, before the $f = 30.0mm$ lens. Another optional iris is placed after the $f = 60.0mm$ lens.

FIGURE 3.6: This helps to form circular apertures of variable radius

IN HERE I MAY TALK ABOU THE M FACTOR, QUALITY PARAMETER OF GAUSIAN BEAMS M^2 Power $200mW$

3.1.4 Waist Lens

After successfully achieving a Gaussian profile, which is important for the reasons described in Section 2.1.2. After the spatial filter, we need a way to control the pump waist, but we need to do it in a way not too complicated, that doesn't imply too many changes in the experimental setup. Putting a lens in the propagation direction with certain focal lenght f will define a zone around the distance f called *Focus depth*[12], where in the middle we find the narrowest point of the beam. The radius of this zone is:

$$W_0 = \frac{\lambda f}{\pi W_B} \tag{3.1}$$

Where W_B is the initial waist beam. In Figure 3.7 we see this behaviour, this zone is produced around the distance f and the radius W_0 is a function of f and W_B. making that if we want to change W_0 we need to use a different lens with f' and also the *Focus depth* will be at a different distance.

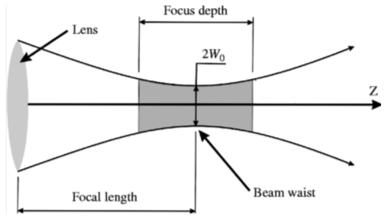

FIGURE 3.7: Effect of lens on a Gaussian beam

If we want to focus the beam at a fixed distance F, using this method to control the pump waist is not practical. Every different lens we would use will make this waist W_0 at a differents distances f. It is necessary to find a *Waist lens* that make us a W_0 at a transverse plane located in a fixed position F from the *Waist Lens*. In Figure 3.8 we present a special lens, consisting in an arrangment of two lenses, a positive and negative one respectively, separated a distance d_0 from each other. Where we can define a *effective focal length F* as

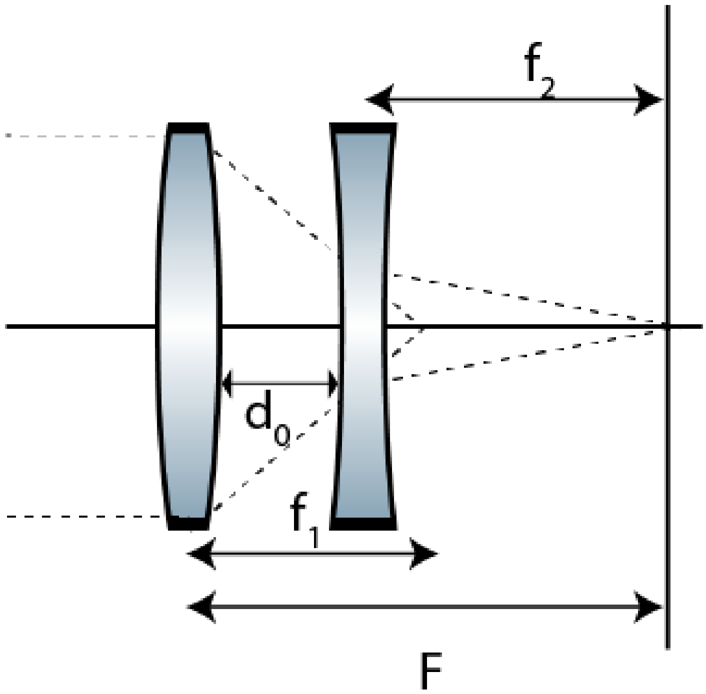

FIGURE 3.8: Composition of lenses to control the Pump Waist at a Fixed distance F

a function of f_1 and f_2, the focal lengths of the positive and negative lenses respectively. With the constrain that $d_0 < f_1$, F reads:

$$F = \frac{f_1|f_2|}{|f_2| - f_1 + d_0}. \tag{3.2}$$

This new effective focal length is crucial in the realisation of this experiment, as described before, we are interested in observing the effect in the reconstructed image using different spatial correlations. This is done by changing the pump waist of the laser that is focused on the crystal. It is not experimentally practical to be changing the crystal position, it would mean to change the position of all the optical elements that follows. For this reason, it is perfect to be able to achieve the desired pump waist just by changing the relative separation of two lenses.

3.1.5 BBO(Beta Barium Borate) Crystal

The Beta Barium Borate (BBO) is an inorganic compound, with chemical formula β-BaB_2O_4. This crystal is a nonlinear optical media commonly used. It is also a birefringent[2] material and its transmission regions extends from $189nm$ to $3500nm$[15]. The type-II crystal is mounted is such way that the input and output plane are fixed, Figure 3.9(a). In particular the input plane is at F from the *waist lens* presented in the previous section, the power of the pump at this point is $\sim 60mW$. In Figure 3.9(b) is a schem of the noncolinear configuration at the output plane of the crystal.

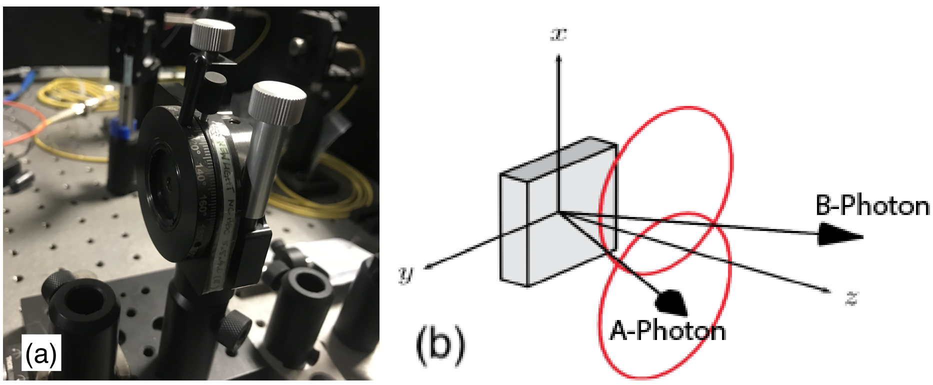

FIGURE 3.9: (a):Actual BBO crystal used in experiment. (b): the noncolinear configuration presented in this experiment

At this point we have as a result of the SPDC process a pair of entangled photons, which have an strong correlation. This correlation is the feature in which we are interested on. We need to observe the shape of this correlations functions and the next section will focus on the experimental setup that will allow us to observe this.

[2]Birefringence is a optical property of some materials of having a refractive index that depends on the polarisation and the propagation of light[12]

3.2 Spatial Correlations Measurement Setup

From this point we will talk about a pair of correlated photons, that will come from the output plane of the BBO crystal, for historical reasons this photons are labeled as *signal* and *idler*. Nevertheless, to keep the same notations used through this monograph, this photon are going to be labeled as A-photon and B-photon, depending on which path they follow, in Figure 3.10 we can see the experimental setup for measuring the spatial correlations, and the different paths the light follows.

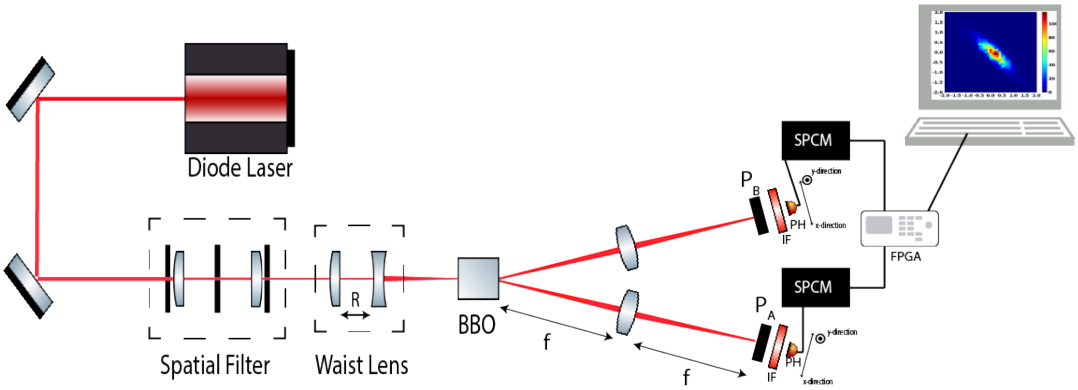

FIGURE 3.10: Experimental Setup for Obtaining the spatial correlations of a pair of down-converted photons

3.2.1 Lens (Fourier Plane)

The next optical element that the pair of correlated photons find in their path is a pair of lenses. This pair of lenses are located at a distance f from the crystal. They define a $2f$ system and place a Fourier plane at a $2f$ distance from the crystal. As discused before, this plane is important because of the relation between the transverse momentum of the light before the 2-f system, and the photon position after de system, Eq. 2.16. We use a lens(LA1708) of $f = 200.0mm$ in front of each A and B.

3.2.2 Polariser

We are interested in just a pair photons, $\Phi(\vec{q}_B, \Omega_B; \vec{q}_A, \Omega_A)$, that are polarised in certain direction. In order to filter the others photons $\Phi(\vec{q}_A, \Omega_A; \vec{q}_B, \Omega_B)$, we place a pair of polarisers at both paths. A polariser is an optical element that filter light, it filters light depending on the direction of the electrical field.

We used a pair of Polarisers(WP25M-UB), which consist of an array of parallel metallic wires sandwiched between glass with certain coating for better transmission.

3.2.3 Interferometer Filter

As pointed out in Section 2.1.2, in order to observe the transverse correlations, the frequency information has to be traced out. For doing so, we placed a pair Interferometer filters. This optical elements have the special feature that only transmits light that comes throught in certain range of frequencies. To do this filtering we used a spectral filter(FB810-10) that only transmits the light that comes with $\lambda = 810 \pm 2nm$.

3.2.4 Detection Module

To observe the spatial correlations we have to be able to measure light that is propagating in the z-direction. Figure 3.11 shows the plane that is being scanned, where each square have a x_i and y_j position, i, j goes from 0 to N. With the help of a motorised translational stages, we can make this N steps. we can control the movement of a pin hole detector, which consists in a single mode optical fiber tip. The translationas stages are controlled by Arduinos, this enable us to do the scan in a complete automated way.

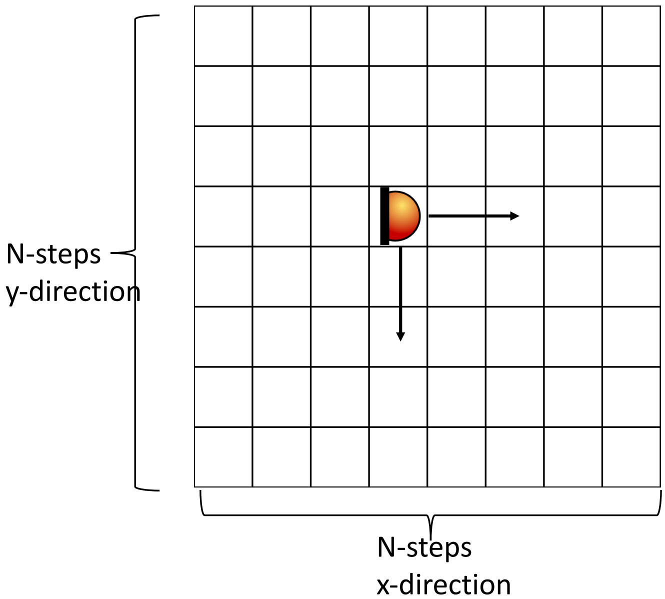

FIGURE 3.11: The plane that is being scanned by the fiber tip, it is a $4x4mm$ square, that can be scanned in N steps, where N is defined by us

Another feature that is easily controlled, is the exposure time. It means we can set how many seconds, is going to be the fiber tip at every (i, j) position. A greater time means more photon counted, and with a bigger amount of data of photons counted per position, the means values per position gives a better image, with better contrast. The places where we don't have photons tend to have a low mean value of photons counted, while the more intense places keep counting, hence having bigger means values. The (i_B, j_B) position and (i_A, j_A) position are related with $\vec{q}_B = (q_i, q_j)$ and $\vec{q}_A = (q_i, q_j)$ in Eq 2.9 $\tilde{\Phi}(\vec{q}_B, \vec{q}_A)$, respectively. The spatial correlation we seek to observe. When taking a Two-photon imaging we already deduce in the previous Chapter that the image is going to be related with $R(\vec{r}_A)$ from Eq. 2.23, where the (i_A, j_A) position is related with $\vec{r}_A = (x_i, y_j)$.

3.2.5 Single Photon Counting Module(SPCM)

Light is transmitted through an optic fiber from the pin hole detector to the SPCM. This consists in a self-contained module that detects single photons of light over the $400nm$ to $1069nm$ wavelength range. The module used is SPCM-AQRH-13, and it uses a unique silicon avalanche photodiode (SLiK) with a detection efficiency of more than 65%[16]. The result signal coming from the SPCM are pulses where each one represents one photon.

FIGURE 3.12: Single Photon Counting Module

3.2.6 Field-programmable gate array(FPGA)

Both A and B pulses from the respective SPCM goes to the same Field-Programmable Gate Array (FPGA). This FPGA (ZestSC1) is programmed to count the photon coincidences, this means that the FPGA is fast enough to detect and separate pulses from photons that are time-separated.

3.2.7 Computer(Data Analysis)

LabvVIEW is used to control the detection module, and also, to recibe and translate the information from the FPGA. It deliver the single and coincidence counts for every position in the scan grid, Fig. 3.11. Using this information is only matter of use any way to handle this data and generate the graph for single and coincidence counts. Through this monograph it has been used the python language and the matplotlib library to generate them.

3.3 Two-Photon Imaging Setup

For the Two-photon imaging process we no longer have spatial information about the B-photon after it interacts with the object. Figure 3.13 shows the experimental setup for this stage of the experiment. It is important to remember that all the setups shown so far, are in esence the same optical elements, It was important to create a Experimental setup that allows us to measure different things without changing to much. In this stage we re-direct the light that goes through the object to a detector D_C.

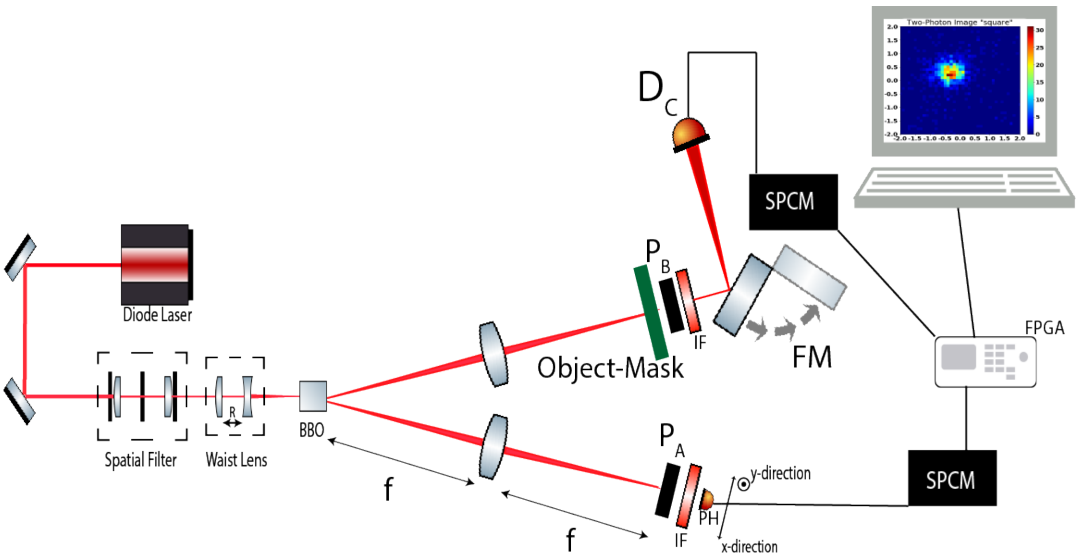

FIGURE 3.13: Experimental Setup for the Two-photon Imaging

3.3.1 Object-Mask

This is an obstruction that is placed in the B path. This is the object from which we will make an image. It consist in an aperture on a translational mount, that allow us to move the aperture precisely in the same plane we make our detections. This is done by manipulating a pair of screws. We used differents objects and in Figure 3.14 there is a detailed schematic of the first one used. It consists in a square aperture placed in the 4th quadrant of the scanned plane.

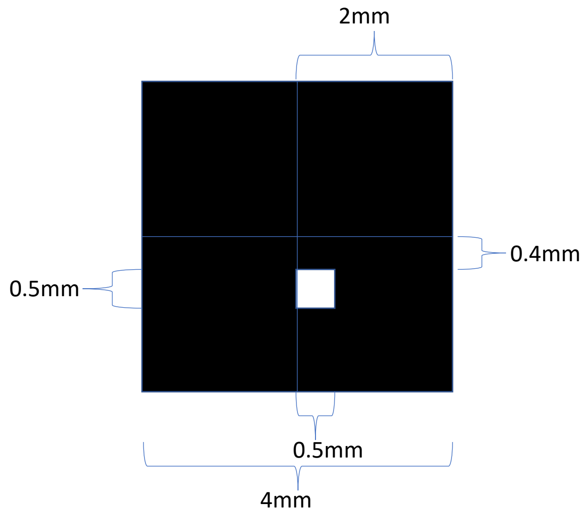

FIGURE 3.14: Detailed description of the "square" aperture location in the scanned plane

In Figure 3.15 there are the other two apertures that we used so far in the experiment, this apertures where selected because of the symmetries and antisymmetries they present, the goal of this monograh is to study the effect of the spatial correlations in the image recovered, effect such as reflection of the original image, quality and others.

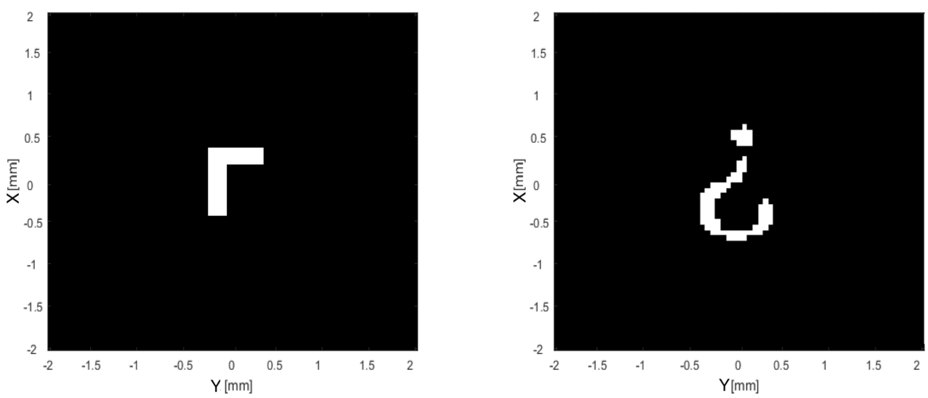

FIGURE 3.15: The other two apertures used

3.3.2 Folding Mirror

In order to change de path followed by the B-photon, and guide the light to a new detector $D_C$we use a Folding mirror, Figure 3.16. This mirror plays the role of a switch, when is up, we are know dealing with the D_C detector, and we are doing a Two-photon Imaging process. In contrast, when the mirror is down, we are recovering spatial information, so it is possible to recognise some sort of shadow from the object, or we are measuring the spatial correlations.

FIGURE 3.16: Foldind Mirror, it is in the position for measuring the correlations

3.3.3 Bucket Detector

This detector consist denominated D_C detector. It is a coupling lens that collects all the light that goes through the object. The lens position is fixed, and it gathers all light and send it to a multi mode optical fiber connected to a SPCM. In contrast to the other detections made before, the Bucket detector loses track of any spatial information of the photons.

Chapter 4

Results

In This chapter we present the experimental data recovered through the diferents steps described in the Chapter before. Most the following results consists in 2-D arrays representing a matrix, where in each position a color is painted, depending on how many photons were detected in single or coincidences counts. As we have seen, before making a Two-photon image, there are some process that have to be made before. The first thing todo is to achieve a Gaussian behavior of the original diode laser. For doing do we have to look at the beam propagation after the Spatial Filter.

4.1 Achiving a Gaussian Beam

PYTHON PROGRAM STILL ON PROGRESS, TALK ABOUT M FACTOR

4.2 Finding The Correlated Photons

After obtaining a Gaussian propagation, and achieve a pump waist that no varies to much while propagates, we focused the laser at the BBO crystal and with the help of the *waist lens* we set the $w_p = 91\mu m$. Before observe the spatial correlations of the down converted photons, we make sure we are seing them. Figure 4.1 shows two different images recovered, where in Fig.4.1(A) we found out that the translational mount of the mask was not well placed, it was cutting some of the light.

In Figure 4.1(B) we can the B-photon, and now there is no interference by the translational mount. As said before we placed a pair of polarisers in order to filter them. In the figure we can see that just one direction of the ring in 3.9(b) while the other is partially filtered.

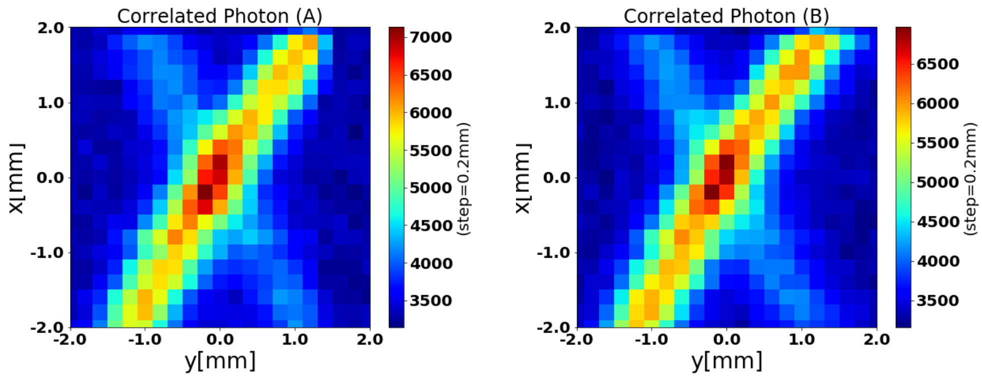

FIGURE 4.1: (A) and (B) shows the B-photon of the down converted pair. In (B) we moved away the translational mount of the mask

4.3 Experimental Correlations

Afterwars we would like to observe the shape of the spatial correlations the pair of down converted photons and see the experimental behaviour of $\tilde{\Phi}(\vec{q}_B, \vec{q}_A)$. When remembering the definition of $\vec{q}_n$, it is a 2-D vector, containing the information of the photon in x and y direction. Since we have two photons, each one with two spatial variables. Resulting that we can 4 differents correlations for a pair of photons. There is important to point out that this transverse momentum $\vec{q}_n$ is related with his equivalent $\vec{r}_n$ the position of the photon, with n making reference to the A and B paths.

In Figure 4.2 there are the correlations in the xx and yy direction. The 2-D matrix in Figure 4.2(*XX Correlation*) is the result of repeating this recipe: placing the D_A at a fixed position and scanning the D_B just in the x direction, next we move de D_A one position in the x direction. Repeating this N times we construct an image of the coincidence counts between D_A and D_B in every position.

Figure 4.2(*YY Correlation*) show the spatial correlation in the yy direction, this image is done by repeating the same recipe as before, but this time scanning and moving in the y direction. The spatial correlations in this case present a negative behaviour in both XX and YY direction, an anticorrelation. Meaning that is expected to measure a photon at a negative position at the B path if we measured a photon at a positive position at the A path. They both exhibit a elliptical shape, but the YY correlation is a narrower one, meaning there is a stronger relation between the pair of photons in the Y direction.

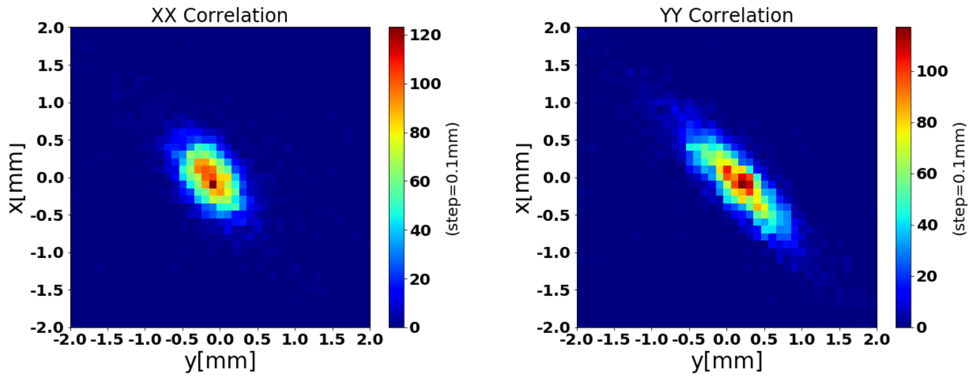

FIGURE 4.2: Experimental Spatial correlations between a pair of down-converted photons. *XX Correlation* shows the correlation in the x variables. *YY Correlation* shows the correlation in the y variables, Beam propagating in the z direction. $w_p = 91\mu m$

4.4 Mask Alignment

Before making a Two-photon image we need to know that we have placed the mask in the correct spot. This correct spot is defined by the Figures 3.14 and 3.15. Which localisation was decided in function of where the flux of correlated photon was greater. The following images where produced as the standar image is done. It means we show the shadow of the aperture in the B path. Every position of the images is the single counts of the D_B in the exposure time. It is like the standar image in the sense that we are using the spatial information of the light that interacted with the mask.

4.4.1 Mask 1

The Following Figure 4.3 shows the final localisation of the first mask used. It was the final position because its position is really similar to the one described in Figure 3.14. For making this image we set the step length to be $0.2mm$ and the exposure time was 1 second per position.

4.4.2 Mask 2

Figure 4.4 shows the localisation of the second mask. While in Figure 4.4(A) there is the initial position of the mask, Figure 4.4(B) shows the new localisation of the aperture after a translation in the y direction. This images where done by setting the steps to $0.2mm$ and the exposure time to 1 second per position.

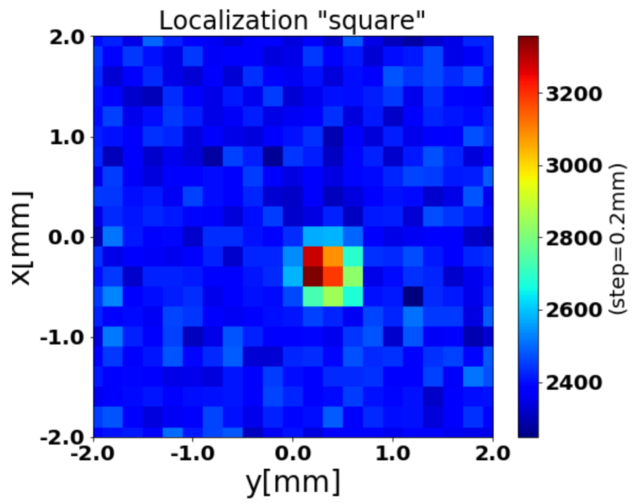

FIGURE 4.3: Localization of the mask with an square

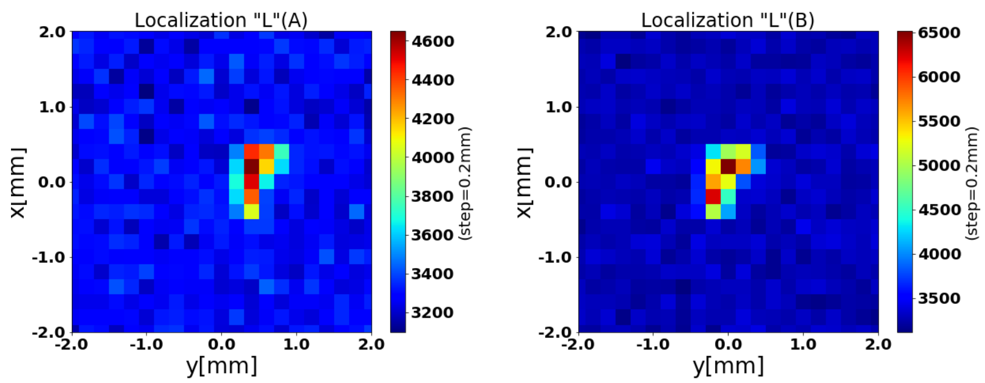

FIGURE 4.4: Moving the L Mask in order to put it in the most central spot

In Figure 4.5 is presented the definitive position of the aperture before making a Two-photon imaging. If we take a closer look to the Figure, we can appreciate a higer contrast, this is because in this opportunity we set the steps to be $0.1mm$ and the exposure time to be 30 seconds per position. This image is the result of measuring for around 14 hours.

4.4.3 Mask 3

The definitive localisation of the third mask used is presented in the Figure 4.6, where the step was $0.1mm$ and the exposure time was set to 30 seconds per position.

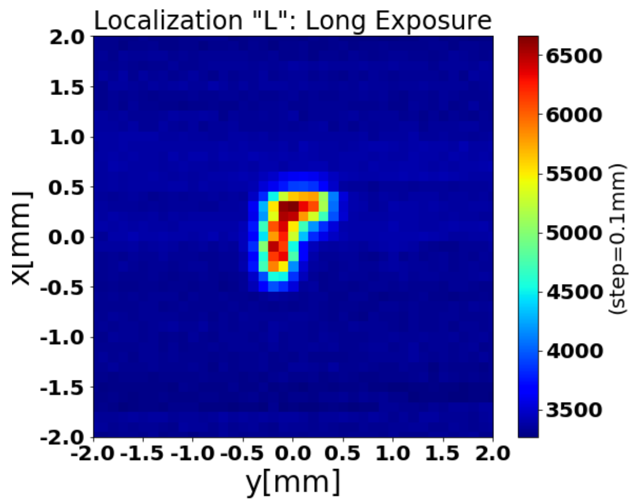

FIGURE 4.5: Long exposure of the definitive localization of the mask, in this try we leave the detector in each place for 30 seconds, we also make the steps of the detector smaller, $0.1mm$

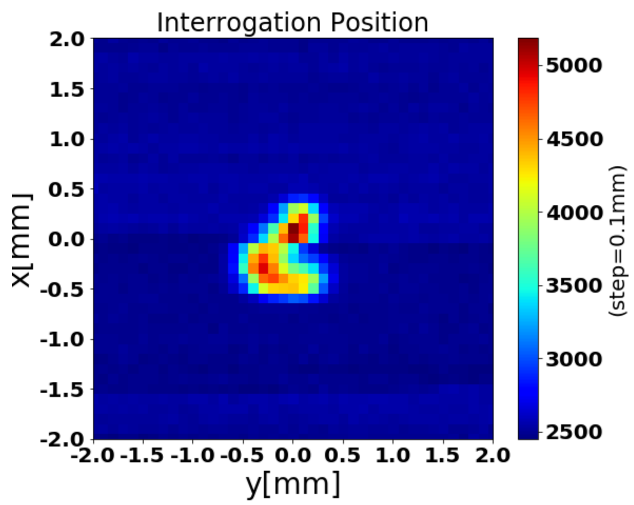

FIGURE 4.6: Interrogation definitive position

4.5 Two-Photon Images

Finally we get to observe the Two-photon images that are the core of this monograh, It is important to remember the way this images are obtained. The image $R(\vec{r}_A)$ is a function of the coincidence counts between D_C and D_A. We scan D_A, and as a result we obtain a 2-D matrix where each (i, j) position is the coincidence count.

4.5.1 mask1

Figure 4.7 is the Two-photon image of the square aperture. The maximun coincidence counts changed position in the image, compared to Figure 4.3. Nevertheless the shape is identificable, still has a shape of square, but its position is reflected in both x and y direction.

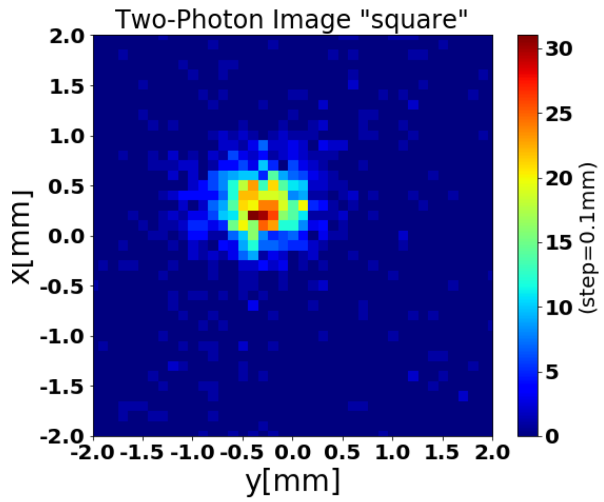

FIGURE 4.7: Experimental Two-photon image recovered for the square aperture

4.5.2 mask2

The Two-photon image of the second mask is presented in Figure 4.8. In this opportunity it is clear that the more complex shape of the aperture is hardly identifiable. However, there are some other interesting things to note about the image. As the original aperture, the image is not symmetrical, and it is not pointing to the original direction the L was in Figure 4.5. This make us to think about reflexions in the image respect from the original mask, but in this case is not that easy to detect them.

4.5.3 mask3

The third Two-photon image is in Figure 4.9. Again the complex original shape is barely visible in the image obtained, Nevertheless the image have a more rounded part at the biger Y position, that hint us about a reflexion of the interrogation symbol, now it is oriented like '?', so it may present a reflexion in both x and y direction.

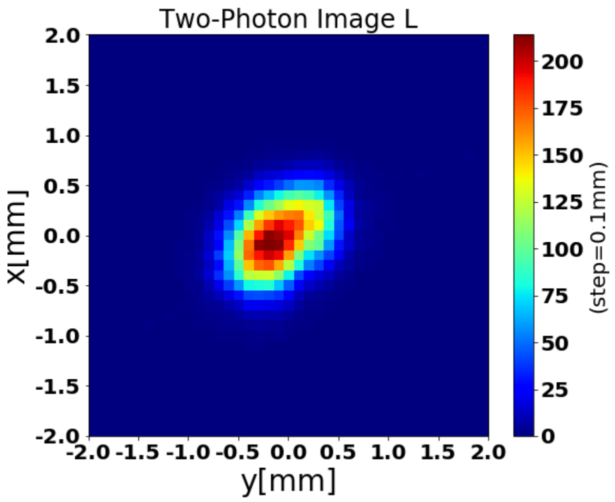

FIGURE 4.8: Two-photon image recovered for the L aperture.

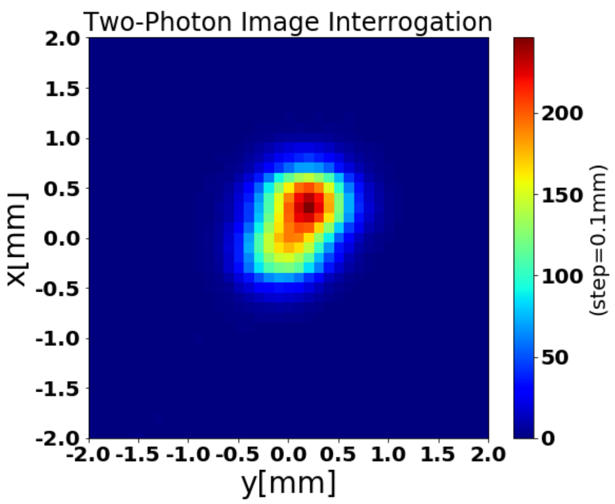

FIGURE 4.9: Two-Photon Image Interrogation

Chapter 5

Discussions and Conclusion

1. signo correlacion relation with the position of the image.... how norrow a spatial correlation and the quality of the resulting image.

2. the entanglement is not a necesary thing, Por otro lado it is import to note that entangled photons can be usefull beause of the strong correlations they can present

3. talk something about thermal Appendix A.

4. what is the true nature of the ability of recotrsucting an image, why correlation light intensities.[6] In summary, we may conclude that ghost imaging is the result of quantum in- terference. Either type-one or type-two, ghost imaging is characterized by a non-factorizable point-to-point image-forming correlation which is caused by constructive-destructive interferences involving the nonlocal superposition of two-photon amplitudes, a nonclassical entity corresponding to different yet indistinguishable alternative ways of producing a joint photo-detection event. The interference happens within a pair of photons and at two spatially separated coordinates. The multi-photon interference nature of ghost imaging determines its peculiar features: (1) it is non- local; (2) its imaging resolution differs from that of classical; and (3) the type-two ghost image is turbulence-free. Taking advantage of its quantum interference nature, a ghost imaging system may turn a local "bucket" sensor into a nonlocal imaging camera with classically unachievable imaging resolution. For instance, using the Sun as light source for type-two ghost imaging, we may achieve an imaging spatial resolution equivalent to that of a classical imaging system with a lens of 92-meter diameter when taking pictures at 10 kilometers.10 Furthermore, any phase disturbance in the optical path has no influence on the ghost image. To achieve these features the realization of multi-photon interference is necessary[17].

Appendix A

Two-photon Imaging Using Chaotic Sources

In principle the term "thermal radiation" should refer only to radiation coming from a blackbody in thermal equilibrium at some temperature T. But with this realisation of thermal radiation we have to face some characteristics of true thermal fields. Thermal radiation is also referred as chaotic light, which have extreme short coherence time. This is because a thermal source contains a large number of independent sub-sources, such as the trillions of atoms or molecules.These atomic transitions that can be identical or different act like sub-sources, that emit light into independently and randomly.

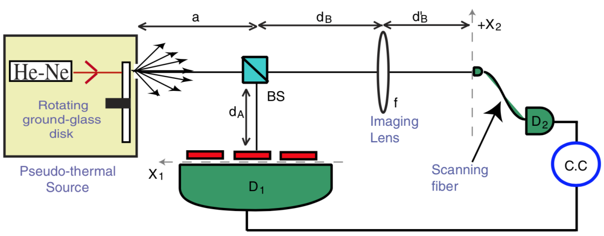

FIGURE A.1: Experimental setup for the Two-photon imaging using thermal light, taken from [3]

The source light in Figure A.1 is the one developed by Martinssen and Spiller[18] which is the most commonly used among the pseudothermal fields. A coherent laser radiation is focused on a rotating ground glass disk, the scattered radiation is chaotic with a Gaussian spectrum. After this, a nonpolarizing beam splitter (BS) splits the radiation in two distinct optical pths, In the reflected arm an object, with transmission function $T(r_1)$, is placed ar a distance d_A from the BSand a bucket detector (D_1) is just behind the object. In the transmitted arm an imaging lens, with focal lenght f, is placed at a distance d_B from the BS, and a multimode optical fiber (D_2) scans the transverse plane at a distance d_B' from the lens. The output pulses from the two single photon counters are sent to an electronic coincidence circuit to measure the rate of coincidence counts.

Once again we expect the joint-detection counting rate between photodetectors D_1 and D_2 to behave like the one described in Eq. 2.13. But thos rate this coincidence counts is governed by the second-order Glauber correlation function [19]:

$$G^{(2)}(\vec{r}_1;\vec{r}_2) \equiv \langle E_1^{(-)}(\vec{r}_1)E_2^{(-)}(\vec{r}_2) \times E_2^{(+)}(\vec{r}_2)E_1^{(+)}(\vec{r}_1)\rangle \tag{A.1}$$

where the $E^{(-)}$ and $E^{(+)}$ are the negative-frequency and the positive-frequency field operators describing the detection events at the locations $\vec{r}_1$ and $\vec{r}_2$. The transverse second-order correlation correlation function for a thermal source is given by [3]:

$$G^{(2)}_{thermal}(\vec{r}_1;\vec{r}_2) \propto \sum_{\vec{q}} |g_1(\vec{q},\vec{r}_1)|^2 \sum_{\vec{q}'} |g_2(\vec{q}',\vec{r}_2)|^2 + |\sum_{\vec{q}} g_1^*(\vec{q},\vec{r}_1)g_2(\vec{q},\vec{r}_2)|^2 \tag{A.2}$$

where $\vec{r}_i$ is the transverse position of the detector D_i, $\vec{q}$ and $\vec{q}'$ are the transverse components of the momentum vectors, and $g_i(\vec{q},\vec{r}_i)$ is the Green's function associated with the propagations of the field with transverse momentum $\vec{q}$ from the source, to the position $\vec{r}_i$ at the detection plane defined by the detector D_i. $g_i(\vec{q},\vec{r}_i)$ is defined in a similar way as in Eq. 2.17.

It is important to note that there are two main differences with respect to the SPDC case: First the presence of a background noise (first term of Eq. A.2), which does not exist for SPDC. Second, the possibility of writing the second term of Eq. A.2 as a product of the first order correlation functions, $G^{(1)}_{12}G^{(1)}_{21}$, while there is no way to write the biphoton produced by the SPDC as a product of other correlations. Also this term $|\sum_{\vec{q}} g_1^*(\vec{q},\vec{r}_1)g_2(\vec{q},\vec{r}_2)|^2$ Is the interference of intensities of a incoherent statistical assemble of randomly distributed photons.

Following the proces done in [3], it can be shown that for any values of distances d_A, d_B and d'_B which obey the equation:

$$\frac{1}{d_B - d_A} + \frac{1}{d'_B} = \frac{1}{f} \tag{A.3}$$

which clearly has the form on a thin-lens equation, defining a point-to-point correspondence between imaging and object plane. Then Eq. A.2 can be simplified as:

$$G^{(2)}_{tot}(\vec{r}_2) \propto N + |T\left(\frac{d_A - d_B}{d'_B}\vec{r}_2\right)|^2 \tag{A.4}$$

where $T(\frac{d_A - d_B}{d'_B}\vec{r}_2)$ is the object transmission function ($T(\vec{r}_1)$) reproduced on the D_2 plane. Thanks to this result we can conclude that a thermal source allows reproducing in coincidence measurements the two-photon image of an object, similarly to the SPDC case, except for a constant background noise, where N is proportional to it.

It is possible to establish an analogy between classical optics and entangled two-photon optics: the two-photon probability amplitude plays in entangled two-photon processes the same role that the complex amplitude of the electric field plays in classical optics [3].

Bibliography

[1] Crystal Laser. Crystal laser. http://www.crystalaser.com. Accessed: 2018-03-09.

[2] Inc. Thorlabs. Thorlabs, inc. https://www.thorlabs.com/index.cfm. Accessed: 2018-03-09.

[3] Alejandra Valencia, Giuliano Scarcelli, Milena D'Angelo, and Yanhua Shih. Two-photon imaging with thermal light. *Phys. Rev. Lett.*, 94:063601, Feb 2005.

[4] T B. Pittman, Yanhua Shih, D V. Strekalov, and Alexander Sergienko. Optical imaging by means of two-photon quantum entanglement. *Physical review. A*, 52:R3429–R3432, 12 1995.

[5] Giuliano Scarcelli, Alejandra Valencia, and Yanhua Shih. Experimental study of the momentum correlation of a pseudo-thermal field in the photon counting regime. *Conference on Lasers and Electro-Optics/Quantum Electronics and Laser Science and Photonic Applications Systems Technologies*, page JTuC122, 2005.

[6] MaLin Zhong, Ping Xu, LiangLiang Lu, and ShiNing Zhu. Resolution of ghost imaging with entangled photons for different types of momentum correlation. *Science China Physics, Mechanics & Astronomy*, 59(7):670311, May 2016.

[7] Lorenzo Basano and Pasquale Ottonello. Experiment in lensless ghost imaging with thermal light. *Applied Physics Letters*, 89(9):091109, 2006.

[8] Omar Calderón-Losada, Jefferson Flórez, Juan P. Villabona-Monsalve, and Alejandra Valencia. Measuring different types of transverse momentum correlations in the biphoton's fourier plane. *Opt. Lett.*, 41(6):1165–1168, Mar 2016.

[9] A. Einstein, B. Podolsky, and N. Rosen. Can quantum-mechanical description of physical reality be considered complete? *Phys. Rev.*, 47:777–780, May 1935.

[10] Clara I Osorio, Alejandra Valencia, and Juan P Torres. Spatiotemporal correlations in entangled photons generated by spontaneous parametric down conversion. *New Journal of Physics*, 10(11):113012, 2008.

[11] Jefferson Flórez, Omar Calderón, Alejandra Valencia, and Clara I. Osorio. Correlation control for pure and efficiently generated heralded single photons. *Phys. Rev. A*, 91:013819, Jan 2015.

[12] E. Hecht. *Optics*. Pearson education. Addison-Wesley, 2016.

[13] Y. Shih. *An Introduction to Quantum Optics: Photon and Biphoton Physics*. Series in Optics and Optoelectronics. Taylor & Francis, 2011.

[14] Morton H. Rubin. Transverse correlation in optical spontaneous parametric down-conversion. *Phys. Rev. A*, 54:5349–5360, Dec 1996.

[15] D. N. Nikogosyan. Beta barium borate (bbo). *Applied Physics A*, 52(6):359–368, Jun 1991.

[16] PerkinElmer. *Single Photon Counting Modules – SPCM*, 2010. Rev. 1.

[17] Jeffrey H. Shapiro and Robert W. Boyd. The physics of ghost imaging. *Quantum Information Processing*, 11(4):949–993, Aug 2012.

[18] W. Martienssen and E. Spiller. Coherence and fluctuations in light beams. *American Journal of Physics*, 32(12):919–926, 1964.

[19] Roy J. Glauber. The quantum theory of optical coherence. *Phys. Rev.*, 130:2529–2539, Jun 1963.